7 Confining and Probing Single Molecules in Synthetic Liposomes

C. F. Wilson, D. T. Chiu, R. N. Zare, A. Strömberg, A. Karlsson, and O. Orwar

As organisms, we are amazingly complex living laboratories. As we move, breathe, think, and eat, seemingly endless chemical reactions and interactions occur inside us. The test tubes, beakers, and flasks used to separate and selectively mix the myriad of reactants involved are cells, vesicles, and organelles. Taking the analogy further, whereas chemists typically mix chemicals milliliters or more in volume, biological systems carry out their biochemistry in containers that are femtoliters or less in volume. As researchers we assume, with good reason, that the material surfaces of our laboratory test tubes do not substantially affect the kinetics we measure. This assumption might not hold were we to shrink our containers to the femtoliter scale. At such a small scale, collision rates between reactants and their container walls become significant [1], and the inner surface, particularly in biological containers, is chemically complex. The bilayers of cells and organelles are composed of a variety of lipids. These varieties assemble into domains [2] in a process partly controlled by the transmembrane proteins in them [3]. Cellular and organellar control of chemical reactions may thus come, in part, from alterations in the composition and arrangement of the molecular species making up the bilayer membrane [4]. How do systematic alterations to the bilayer composition of a liposome alter the kinetics of reactions within the liposome interior? We may find that the potential physiological significance of lipid domains within bilayers to the kinetics of in-plane reactions [5] (i.e., for proteins and other molecules moving within the bilayer) has applications to molecules within liposomes that interact with the inner bilayer surface.

A method for investigating these questions has been elusive. The challenge is to make, manipulate, and mix the contents of biomimetic containers for biochemical studies in the laboratory. Our approach is to use synthetic liposomes (vesicles) to carry out chemistry on the femtoliter scale, with the specific aim of studying single-molecule kinetics in a biorelevant nanoenvironment.

In the past we have carried out work in the area of solution-phase single-molecule detection [6,7] and manipulation [8,9] as well as single liposome [10] and organelle [11] manipulation and analysis. We developed a protocol in which liposomes are formed at room temperature in two minutes in order to minimize the denaturing and degradation of biological molecules [12].

R. Rigler et al., *Single Molecule Spectroscopy*

We have used these liposomes as chemical containers and reaction vessels for both large numbers of molecules and for single enzymes [1,13]. To improve the protocol used in these experiments, we developed a micropipette capable of holding for over an hour lipid vesicles one to ten micrometers in diameter with little or no change in the suction applied at the micropipette tip and with minimal liposome deformation at the docking point. One-micron-diameter vesicles match well the probe volume of many single-molecule detection (SMD) schemes. The micropipette allows the liposome to be mechanically held in the probe region of a laser beam so that studies can be made of the molecules confined within the liposome. The use of liposomes also allows for the addition of reagents to their interiors to initiate reactions by electroporation or by fusion, for example.

The power of single-molecule studies comes from their ability to detect physical processes that would otherwise be hidden within the ensemble averaging of bulk measurements. The individual steps and chemical intermediates of physical processes can be detected, and the static (between molecules) and dynamic (for a single molecule) heterogeneities contributing to ensemble measurements can be discerned [14]. Exciting evidence for conformational changes of single molecules has been provided by localizing molecules in agarose gel [15], in capillaries [16], in microwells [17], and on glass slides [18,19] or by observing them directly in solution [20,21].

Lu et al. [15], for example, demonstrated that individual cholesterol oxidase molecules turn over substrate molecules with a time-varying rate (on the order of seconds). Over longer periods of time, and for ensembles of cholesterol oxidase molecules, standard kinetics are followed.

Where molecules do not act differently from one another, the same statistics used to describe the ensemble can be used to describe the individual molecular processes therein. Differences might become quite significant where molecules have complex internal structures (such as those leading to conformational changes) or exist within a complex microenvironment (such as in a cell) [22]. To address this latter scenario, we have carried out Monte Carlo simulations of single-molecule Brownian dynamics. These calculations estimate the collision frequencies between individual molecules within a liposome and between those molecules and the inner liposome wall. In addition, we have performed experiments in individual vesicles in which we monitor the turnover rate of substrate molecules by an enzyme [1,13]. In this chapter we review these results, discuss their implications, and report on our related work aimed at exploiting liposomes as tools to look at single molecules and low concentrations of molecules.

Computer simulations were done to estimate the collision frequencies between a substrate molecule (S, with radius r_S), an enzyme molecule (E, with radius r_E), and the inner wall of the vesicle containing them [1]. The substrate was fluorescein diphosphate and the enzyme alkaline phosphatase to correlate with our experimental work. For simplicity, each molecule was

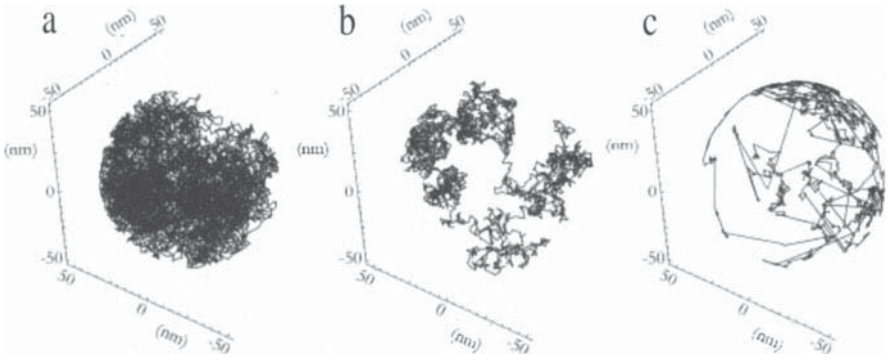

Fig. 7.1. Trajectories of (**a**) a single substrate and (**b**) a single enzyme inside a 104-nm diameter sphere modeled using a Brownian dynamics Monte Carlo simulation. The substrate was followed for 10^4 steps with 10 ns between each step, and the enzyme for 2.5×10^3 steps with 40 ns between each step. (**c**) A trace showing collisions between a single substrate and the spherical wall (40 x 10^6 steps with 1.5 ps between steps). Reprinted from Chemical Physics, vol. 247, Chiu et al., "Manipulating the biochemical nanoenvironment around single molecules contained within vesicles," pp. 133–139, 1999, with permission from Elsevier Science

modeled as a sphere and the vesicle as having hard walls. A collision occurs between S and E when they are within the distance $r_{SE} = r_S + r_E$. The radii were estimated from the Stokes–Einstein equation by using diffusion coefficients of molecules of similar masses. For the enzyme and substrate we took respectively $D_E = 7 \times 10^{-11}$ m^2/s and $D_S = 4.4 \times 10^{-10}$ m^2/s. The Stokes–Einstein equation does not account for charge effects, and it is most applicable to solute molecules that are large compared to the solvent molecules. Consequently, this approximation probably introduces inaccuracies for r_S [23]. The effective charge and size of S will be reduced and increased, respectively, by S's solvation. Both these effects act to improve the accuracy of the calculation. For these reasons, as well as for simplicity, we use the Stokes–Einstein approximation for r_S.

Each molecule (S and E) within the vesicle was allowed to move a random distance in each step. The random displacement lengths were uniformly distributed between maximum displacements in both directions for each dimension. The time step, Δt, needed for the simulation is chosen so that the diffusion coefficient calculated from it ($D = \langle x_n^2 \rangle / 2n\Delta t$) reproduces the estimated values for D_S and D_E. The maximum displacements used for S and E were kept roughly the same, making each time step for S one-fourth as long as that for E. This difference in time steps reflects the fact that D_S is larger than D_E and allows for a simulation in which the solvent affects the diffusive path more for S than for E.

Figures 7.1a and b show traces of the diffusive paths followed by S and E, respectively, within a 104-nm diameter sphere in 100 μs. Figure 7.1c is

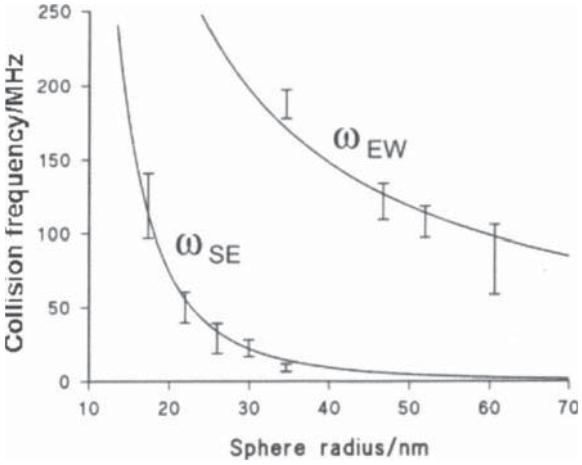

Fig. 7.2. A plot showing collision frequency vs. vesicle radius r. ω_{SE} is the substrate–enzyme collision frequency (40×10^6 steps with 1.5 ps between steps), and ω_{EW} is the enzyme–wall collision frequency (10×10^6 steps with 6 ps between steps). To demonstrate the volume and radius dependence of collision rates respectively ω_{SE} and ω_{EW} vs. r were fit to the function $y = kx^{-r}$. For ω_{SE} $r = -3$ (correlation coefficient = 0.997) and for ω_{EW} $r = -1$ (correlation coefficient = 0.999). Reprinted from Chemical Physics, vol. 247, Chiu et al., "Manipulating the biochemical nanoenvironment around single molecules contained within vesicles," pp. 133–139, 1999, with permission from Elsevier Science

a trace of the collisions between S and the spherical wall over 60 μs [1]. Figure 7.2 plots the collision frequency between S and E (ω_{SE}) and between E and inner sphere (vesicle) wall (ω_{EW}) versus vesicle size [1]. In a 170-nm diameter sphere, ω_{SE} is 0.3 MHz, ω_{EW} is above 50 MHz, and ω_{SW} (the frequency at which S collides with the wall) is 200 MHz. Thus, the single-molecule collision rates for E and S with their container wall are respectively, in a 170-nm sphere, over 150 and almost 1000 times as frequent as the rates of their collisions with each other. Our simulation assumed a perfectly reflective boundary, not taking into account any chemical interactions (from charge or hydrophobic effects, for example). Including such effects could strongly bias where the molecules reside. While some groups of molecules may be repelled from the liposome wall, which would raise their effective concentration in the center of the liposome, others may be biased to spend significant periods near the wall each time they collide with it. If both molecules involved in a reaction spend sufficient time near the bilayer wall, most of their reactions might occur there. Molecules diffusing in two dimensions are more likely to collide than those diffusing in three [24].

Figure 7.3 shows the number of collisions occurring between E and S in a 60-nm sphere over a 60-μs simulation time [1]. The collisions occur in clusters because once a collision occurs, the two molecules remain in the

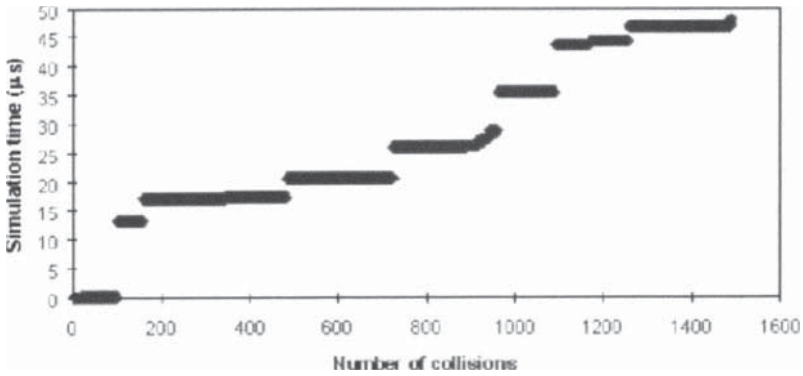

Fig. 7.3. Number of substrate–enzyme collisions during a 60-μs simulation. The vesicle diameter was 60 nm. Reprinted from Chemical Physics, vol. 247, Chiu et al., "Manipulating the biochemical nanoenvironment around single molecules contained within vesicles," pp. 133–139, 1999, with permission from Elsevier Science

same region for some time. This localization makes subsequent collisions more likely. There appears to be no correlation in time between collision clusters. Based on this behavior alone, reactions requiring multiple collisions could be expressed by non-Poissonian rate distributions if they occur within the same collision cluster. Poissonian rate distributions assume random events uncorrelated in time.

To investigate relative reaction rates over time within liposomes, we loaded into liposomes fluorescein diphosphate (from Molecular Probes, Leiden, Netherlands) and alkaline phosphatase (from Sigma). Extravesicular analytes were removed using a size-exclusion column. The liposomes were manipulated using an optical trap, and molecules inside the liposome were detected using laser-induced fluorescence (LIF). The optical trapping and LIF experimental setup have been described elsewhere [1,13]. Briefly, the near-IR light from a MOPA diode laser was sent through a microscope objective to trap the liposome containing the molecules to be studied. An argon ion laser (488-nm line) was then used to excite the enzyme–substrate reaction product (fluorescein). The fluorescence photons were sent through a pinhole via the microscope objective and collected on a single-photon-avalanche diode detector. The starting concentration of fluorescein diphosphate (at the time the liposomes were made) was 0.75 mM. The enzyme concentration was sufficiently low that only one to a few enzymes would be expected to reside inside each liposome. This number varies from vesicle to vesicle and depends strongly on vesicle size and encapsulation efficiency.

Figure 7.4 shows the fluorescence intensity versus time of the enzyme–substrate reaction inside a 3-μm (left) and a 1-μm (right) diameter liposome [1]. Every 60 seconds the reaction product formed was simultaneously probed to measure the fluorescence intensity and photobleached to reset the reaction

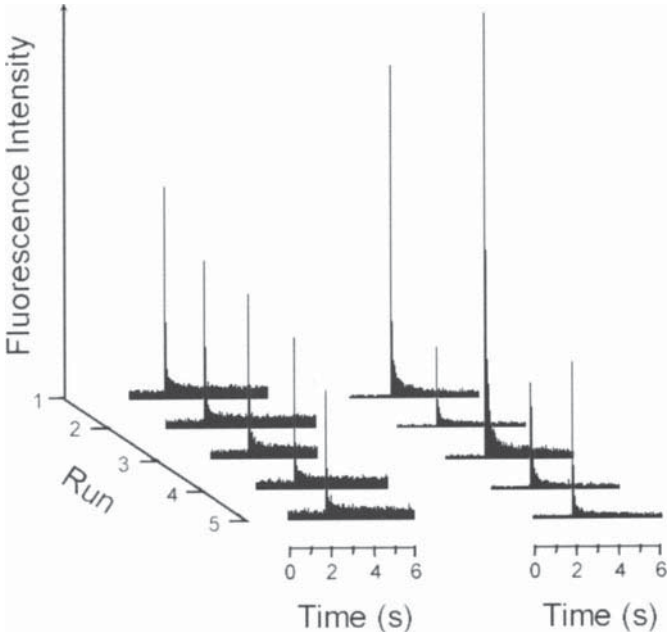

Fig. 7.4. Fluorescence intensity vs. time as a measure of alkaline phosphatase catalytic activity inside an optically trapped vesicle. The substrate, fluorescein diphosphate, was co-encapsulated with the enzyme within the vesicle. At 60-s intervals, the amount of fluorescent product accumulated was simultaneously probed and bleached at 488 nm. The bleaching resets the reaction clock for each run. The vesicles used had radii of 1.5 µm (*left panel*) and 500 nm (*right panel*). Reprinted from Chemical Physics, vol. 247, Chiu et al., "Manipulating the biochemical nanoenvironment around single molecules contained within vesicles," pp. 133–139, 1999, with permission from Elsevier Science

clock. In this way, the relative catalytic activity of alkaline phosphatase was measured every minute over several minutes. In the 3-µm vesicle this activity was nearly homogeneous in time, in stark contrast to the nonhomogeneous product formation in the 1-µm vesicle. While the reasons for the difference are unknown, in the case of alkaline phosphatase the cause of the anomalous substrate turnover rates is unlikely to be conformational changes on the order of minutes [25] (the time scale of each of our experiments), unless bilayer-wall effects cause such changes [26]. In another 3-µm vesicle the turnover rate decreased exponentially with time over a period of 9 minutes [13]. This exponential decrease would be expected for a system in which the substrate concentration has been reduced to the point where diffusion no longer replaces substrate molecules as fast as the enzyme can turn them over.

The experiments just described can be improved by reducing the use of laser light, by sequentially delivering reactants to the liposome while it is held

in the probe volume, and by extending the time over which the measurements are carried out. All these goals can be obtained by holding the liposome with a micropipette.

The use of a micropipette to hold the liposome in the laser probe volume reduces or eliminates the need for an optical trap. The time it takes to dock a liposome to the micropipette tip is typically less than one minute. If liposomes are allowed to settle on a slide (coated with poly-L-lysine or another agent to reduce potential liposome leakage) the liposome can be docked to the micropipette tip without an optical trap. Restricting the use of the trap to a minute or less will reduce or eliminate potential photodamage caused to the biological molecules under study [27]. We have recently developed methods by which reagents can be mixed within individual liposomes. In this procedure microelectrodes are used to electroporate individual cells and organelles [28] or electrofuse individual vesicles [13] and/or cells [29] together. Because these protocols are for individual liposomes or pairs of liposomes, the microelectrodes used to create the electric fields are quite close to (microns), or even in contact with, the liposomes whose contents are to be chemically altered. Consequently, optical traps cannot be used during the electroporation or electrofusion step. The microelectrodes rapidly absorb sufficient light from the trap to form bubbles in the water immediately surrounding them [30]. Any liposomes in the vicinity move away from the microelectrodes quite rapidly. To overcome this problem, we have been working with liposomes that adhere to the surface of glass slides or that are held on the ends of micropipettes. In either case the liposomes are placed, or docked, by the use of optical traps, but those traps are then turned off before positioning the microelectrode tips. In our work with single enzymes, described above, we held onto the liposomes containing the enzyme and substrate molecules with an optical trap, because placing liposomes on slides can in some instances result in liposome leakage, and holding them at the tips of micropipettes has proven to be difficult. Micropipettes capable of providing robust support for a micron-sized liposome would not only facilitate a reduction or elimination in the use of an optical trap but also allow for the introduction of reagents or substrate molecules into the liposome by electroporation or fusion after the liposome is placed into the LIF probe volume. The amount of reactants that is required as a whole would be much reduced, lessening or eliminating the need for a photobleaching event to start the reaction clock in kinetics experiments (again reducing potential photodamage).

We report here the development of micropipettes with tips characterized by a narrow inside diameter (i.d.) and a large liposome-seating surface. The small-tip i.d. (less than one micron) prevents the vesicle from going inside the micropipette. The large liposome-seating surface provides mechanical stability during electroporation, electrofusion, and long-duration (over an hour) experiments for one-to-ten micron vesicles. The seating surface surrounding the tip opening is funnel-shaped so that a liposome can be docked there with-

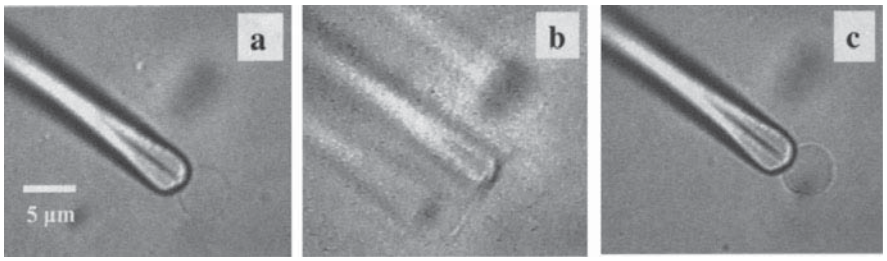

Fig. 7.5. Flick test. Image **a** shows a liposome docked onto a pipette whose inner-tip surface is funnel-shaped. Image **b** showns the liposome and pipette 0.1 seconds after the flick-test impulse is delivered to the manipulator holding the pipette. Several flick tests were performed in rapid succession. The liposome and pipette oscillate at greater than 30 Hz (the video collection rate) with an initial back-and-forth displacement of 20 microns. The oscillation is essentially damped out in 2 s. Image **c** is 3 s after the fourth flick test. No visible instability of the liposome on its seating surface occurs. Application of a small increase in pressure inside the pipette followed by a milder version of such a test allows the liposome to be undocked (see text)

out significant deformation of its surface curvature. Suction and pressure – to dock or undock a liposome, respectively – are provided to the micropipette tip by a system of syringes (10 µL for fine control and 100 µL for coarse control, part numbers 80065 and 81320, respectively, Hamilton, Reno, NV). The syringe plungers are translated by rotating 127-thread-per-inch adjustment screws (part no. AJS127-0.5, Newport Corp., Irvine, CA). The ends of the adjustment screws push against the plunger heads. When a screw is retracted to generate suction, a spring around the associated syringe's plunger barrel pushes the plunger against the screw. Ultrafine pressure control is obtained by the installation of a piezoelectric stack (part no. AE0505D08, Thorlabs, Inc., Newton, NJ) between the 10-µL syringe plunger and its associated control screw. The system uses water as the hydraulic medium, and a 5-mL syringe is installed to act as a reservoir for filling the fine and coarse control elements.

Figure 7.5a shows a 5-µm vesicle docked on a holding micropipette with a 4-µm outer diameter (o.d.) and a 0.5-µm i.d. The micropipette appears to be round where the liposome is seated owing to the extended, round upper lip of the funnel opening. If the line of the vesicle boundary is followed, the vesicle is seen to be seated in the funnel with a small deformation or bud extending into the funnel itself. Each funnel shape corresponds to a particular vesicle size. In this case the micropipette would more naturally hold a smaller vesicle, perhaps 3 µm in size. The extent to which a vesicle deforms into the seating surface is precisely controlled with the fine-pressure syringe (use of the piezo is not necessary for this). To test the mechanical stability of the docked vesicle on the micropipette tip, a "flick test" is performed.

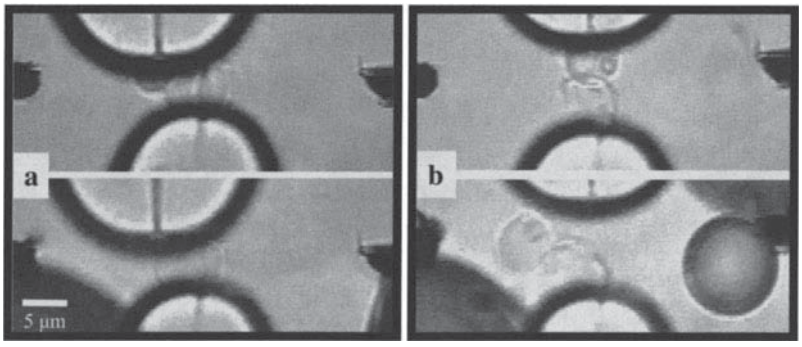

Fig. 7.6. A pair of vesicles is oriented with their lipid bilayers at the point of contact (**a**, top) perpendicular and (**b**, top) parallel to applied electric field lines. The black tips of the microelectrodes used to generate the field are visible on the left and right of each panel. After an electric-field pulse, the perpendicular orientation results in fusion (**a**, bottom) whereas the parallel orientation does not (**b**, bottom)

This test, shown in Fig. 7.5b, consists of literally flicking with one's finger the micromanipulator that is holding the micropipette. In the trial shown, the initial vibration of the micropipette moves the vesicle back and forth over a distance of 20 µm at a frequency of greater than 30 Hz (the video collection rate). The motion is effectively damped out in 2 seconds. Several flick tests were done in rapid succession. Figure 7.5c shows the vesicle after the last test in the series, approximately 10 s after Fig. 7.5a and 9 s after Fig. 7.5b. Using a different vesicle, we did three series of flick tests over 1/2 hour (initially, after 1/4 hour and after 1/2 hour) with similar results. No alterations in suction pressure were needed, and no change in vesicle size was seen. Immediately following the final series of flick tests, the pressure inside the micropipette was increased using the fine-pressure control. A subsequent flick test (of milder nature than shown in Fig. 7.5, consisting of two flicks) jarred loose and then released the vesicle from its seat. It slowly drifted through the field of view and could easily have been optically trapped for subsequent manipulation. We anticipate that for work involving unilamellar liposomes, which are very difficult to optically trap, this micropipette design will offer a stable mechanical method of manipulation.

Figure 7.6 demonstrates vesicle-fusion attempts using microelectrodes (tips seen on the far left and right of each image) and holding micropipettes (tips seen on the top and bottom of each image). These images were taken before we developed a technique to reduce the micropipette tip o.d. (compare them with the more recently designed micropipettes in Fig. 7.5). In Figs. 7.6a (top) and b (top), vesicles are held together so that the plane of their bilayers where they touch are nearly perpendicular or parallel, respectively, to the field lines generated by the microelectrodes. When an electric-field pulse is applied, the electrolysis of water in the region of the microelectrode tips

produces bubbles. These bubbles are seen as large dark spheres extending off the field of view in Figs. 7.6a (bottom) and b (bottom). If fusion does not occur, one or both of the vesicles can be jarred from their micropipette seats as a result of the rapid flow patterns produced by the bubbles. The perpendicular configuration (again referring to the vesicle bilayers where they contact relative to the applied electric-field lines) used in Fig.7.6a and our other work [13,29] results in fusion. Multiple attempts to fuse two vesicles in the parallel configuration, one of which is shown in Fig. 7.6b, were not successful. The trials in Figs. 7.6a and b were done within ten minutes of each other using vesicles from the same drop of solution placed on the microscope stage and used the same micropipettes, microelectrodes, voltage, and pulse-length settings. Thus, the only effective difference between the trials was the configuration of the vesicles with respect to each other and the microelectrodes. The mechanism of electrofusion is not completely understood but may be directly related to electroporation [31–34]. Electroporation occurs in a cell's bilayer membrane predominantly where applied electric-field lines are perpendicular to the cell's surface [35]. The fusogenicity of cells in the perpendicular as compared to the parallel configuration was demonstrated by Tessié and Blangero in 1984 [36]. The use of micropipettes that hold liposomes in a robust way has facilitated our observing the vectoral character of electrofusion on liposomes directly in real time.

Micropipettes with fine-pressure control have been used previously in other applications. For example, micropipettes have been employed to measure the elastic properties of a wide range of bilayer compartments [37], the strength of adhesion between cells [38], and the strengths of interactions between biomolecules bound to liposome surfaces [39]. Sensitive micropipette systems have also been used as tools to build nanoscale biomembrane conduits [40] and to investigate how mechanical stress affects cellular cytoskeletal rearrangements [41], liposome electroporation [42], liposome surface topology [43], and the redistribution of membrane components in cells [44]. Submicrometer-i.d. micropipettes were used to investigate the properties of the membrane cortex of cells as well as to help validate the existence of such a cortex [45]. These various applications differ from those described in our work in that they involve bilayer deformation, often to measure physical properties. Our goal, in contrast, has been to hold liposomes on a micropipette tip with a large funnel-shaped seating surface and a small i.d. to minimize liposomal deformation into the micropipette. Further improvements to the micropipette from those shown here have recently been applied to sensitive (single-digit pN force control) but robust manipulationsof single cells and liposomes as small as 1μm in diameter [46]. Using light scattering, vibration rates of holding micropipettes during flick tests has been shown to average ∼125 Hz, corresponding to holding forces in excess of 2000 pN for some liposomes [46].

The flick test, undocking, and fusion-orientation experiments were done to test the integrity of the recently developed micropipette system. What

lies ahead are many experimental opportunities afforded by the ability to dock, hold, move in three dimensions, electroporate, electrofuse, and undock lipsomes. These opportunities include not only single-molecule studies but also efforts in single organelle and cell manipulation (mechanical, chemical, and genetic). We believe that the use of liposomes as single-molecule containers will provide a strong complement to other techniques as answers are sought to the ever-expanding biochemical complexity that lies before us. The microenvironments surrounding single biomolecules are integral to that expanding complexity. Analysis taking different aspects of *in vivo* conditions into account will provide an improved perspective on the living laboratories of which those single molecules are a part.

References

1. D. T. Chiu, C. F. Wilson, A. Karlsson, A. Danielsson, A. Lundqvist, A. Strömberg, F. Ryttsén, M. Davidson, S. Nordholm, O. Orwar, R. N. Zare, Chem. Phys. **247**, 133 (1999)
2. See, for example, E. J. Shimshick, H. M. McConnel, Biochem. **12**(12), 2351 (1973) entitled "Lateral Phase Separation in Phospholipid Membranes"; J. Korlach, P. Schwille, W. W. Webb, G. W. Feigenson, PNAS-USA **96**, 8461 (1999) demonstrating the exact superposition of like phase domains in the outer and inner leaflet of three-component synthetic vesicles; J. Hwang, L. A. Gheber, L. Margolis, M. Edidin, Biophys. J. **74**, 2184 (1998) entitled "Domains in Cell Plasma Membranes Investigated by Near-Field Scanning Optical Microscopy", A. Rietveld, K. Simons: Biochim. Biophys. Acta. **1376**(3), 467 (1998) entitled "The Differential Miscibility of Lipids as the Basis for the Formation of Functional Rafts." For a discussion of how lipid domains change over a cell cycle for the bacterium *Micrococcus luteus*, see M. Welby, Y. Poquet, J. F. Tocanne, FEBS Lett. **384** (2), 107 (1996)
3. See for example J. Tocanne, L. Cézanne, A. Lopez, B. Piknova, V. Schram, J. Tournier, M. Welby, Chem. Phys. Lipids **73**, 139 (1994); M. B. Sankaram, D. Marsh, L. M. Gierasch, T. E. Thompson: Biophys. J. **66**(6), 1959 (1994); S. Morein, E. Standberg, J. A. Killian, S. Persson, G. Arvidson, R. E. Koeppe II, G. Lindblom, Biophys. J. **73**(6), 3078 (1997); V. Schram, T. E. Thompson, Biophys. J. **72**(5), 2217 (1997)
4. Cells alter their bilayer-lipid composition in response to temperature changes to achieve a particular phase state in their bilayer [E. F. Terroine, C. Hatterer, P. Roehrig, Bull. Soc. Chim. Biol. **12**, 682 (1930); E. R. L. Gaughran: J. Bacteriol. **53**, 506 (1947); A. G. Marr, J. L. Ingraham, J. Bacteriol. **84**, 1260 (1962)]. The phase state achieved corresponds to a very narrow temperature band and results in an anomalously high diffusion coefficient for a probe molecule in bilayers formed from total lipid extracts of *E. coli* at the specific temperatures at which different *E. coli* groups were grown [A. J. Jin, M. Edidin, R. Nossal, N. L. Gersheld, Biochem. **38**, 13275 (1999)]. Corresponding critical states in synthetic bilayers have been shown to provide for unusual mechanical properties [N. L. Gershfeld, L. Ginsberg, J. Membr. Biol. **156**(3), 279 (1997)] and an anomalous heat capacity [N. L. Gershfeld, C. P. Mudd, K. Tajima, R. L. Berger,

Biophys. J. **65**, 1174 (1993)]. Thus, the bilayer membranes of cells have special structural properties very sensitive to small changes in temperature and their protein and lipid composition. The existence of domains within lipid bilayers in living systems is an indication of tremendous phase complexity under cellular control.

5. T. E. Thompson, M. B. Sankaram, R. L. Biltonen, D. Marsh, and W. L. C. Vaz, Mol. Membr. Biol. **12**, 157 (1995)
6. S. Nie, D. T. Chiu, and R. N. Zare, Science **266**, 1018 (1994)
7. S. Nie, D. T. Chiu, and R. N. Zare, Anal. Chem. **67**, 2849 (1995)
8. D. T. Chiu and R. N. Zare, J. Am. Chem. Soc. **118**, 6512 (1996)
9. D. T. Chiu and R. N. Zare, Chem. Eur. J. **3**(3), 335 (1997)
10. D. T., Chiu, A. Hsiao, A. Gaggar, R. A. Garza-López, O. Orwar, and R. N. Zare, Anal. Chem. **69**, 1801 (1997)
11. D. T. Chiu, S. J. Lillard, R. H. Scheller, R. N. Zare, S. E. Rodriguez-Cruz, E. R. Williams, O. Orwar, M. Sandberg, and J. A. Lundqvist, Science **279**, 1190 (1998)
12. A. Moscho, O. Orwar, D. T. Chiu, B. P. Modi, and R. N. Zare, PNAS-USA **93**, 11443 (1996); This paper claimed that most of the vesicles made were unilamellar. Subsequent work (O. Orwar and coworkers, unpublished), has shown that although some of the liposomes produced by this technique are unilamellar, most are multilamellar.
13. D. T. Chiu, C. F. Wilson, F. Ryttsén, A. Strömberg, C. Farre, A. Karlsson, S. Nordholm, A. Gaggar, B. P. Modi, A. Moscho, R. A. Garza-Lopéz, O. Orwar, and R. N. Zare, Science **283**, 1892 (1999)
14. X. S. Xie and H. P. Lu, J. Biol. Chem. **274**, 15967 (1999)
15. H. P. Lu, L. Xun, and X. S. Xie, Science **282**, 1877 (1998)
16. Q. Xue and E. S. Yeung, Nature **373**, 681 (1995)
17. W. Tan and E. S. Yeung, Anal. Chem. **69**, 4242 (1997)
18. T. Ha, A. Y. Ting, J. Liang, W. B. Caldwell, A. A. Deniz, D. S. Chemla, P. G. Schultz, and S. Weiss, PNAS-USA **96**, 893 (1999)
19. L. Edman, Z. Földes-Papp, S. Wennmalm, and R. Rigler, Chem. Phys. **247**, 11 (1999)
20. L. Edman, Ü. Mets, and R. Rigler, PNAS-USA **93**, 6710 (1996)
21. M. Borsch, P. Turina, C. Eggeling, J. R. Fries, C. A. Seidel, A. Labahn, and P. Graber, FEBS Lett. **437**, 251 (1998)
22. C. Bai, C. Wang, X. S. Xie, and P. G. Wolynes, PNAS-USA **96**, 11075 (1999)
23. D. Ermak, J. Chem. Phys. **62**, 4189 (1975)
24. For multicomponent bilayers, reactant molecules might associate differently with different lipid domains. In that case the two-dimensional diffusion of a molecule interacting with the bilayer wall might undergo complex variations. Restricted, time-dependent diffusion has been observed for proteins in cell membranes [see T. J. Feder, I. Brust-Mascher, J. P. Slattery, B. Baird, and W. W. Webb, Biophys. J. **70**, 2767 (1996)] as well as for molecules that associate with transmembrane proteins [R. Simson, B. Yang, S. E. Moore, P. Doherty, F. S. Walsh, and K. A. Jacobson, Biophys. J. **74**, 297 (1998); P. R. Smith, I. E. G. Morrison, K. M. Wilson, N. Fernández, and R. J. Cherry, Boiphys. J. **76**, 3331 (1999)]. Diffusion coefficients for green fluorescent protein (GFP) molecules and derivitized GFP molecules within *E. coli* cells cannot be explained by a single effective cytoplasmic viscosity [M. B. Elowitz, M. G. Surette, P. Wolf, J.

B. Stock, and S. Leibler, J. Bacteriol. **181**, 197 (1999)]. Cytoplasmic diffusion likely varies due to a combination of bilayer wall, cytoskeletal, and other effects.
25. D. B. Craig, E. A. Arriaga, J. C. Y. Wong, H. Lu, and N. J. Dovichi, J. Am. Chem. Soc. **118**, 5245 (1996)
26. *In vivo* alkaline phosphatase activity can be influenced by the phase state of nearby lipid bilayers. See V. M. Bresler, S. N. Valter, M. A. Jerebtsova, V. V. Isayev-Ivanov, E. N. Kazbekov, A. R. Kleiner, Y. N. Orlov, I. A. Ostapenko, A. T. Suchodolova, and V. N. Fomichev, Biochim. Biophys. Acta **982**, 288 (1989); A. S. Molina, A. Paladini, and M. S. Gimenez, Horm. Metab. Res. **29**(4), 159 (1997).
27. Biological molecules transparent to the wavelength used for optical trapping do not undergo photodamaging processes while in an optical trap. Complex systems, especially within living systems, are susceptible to damage over the entire trapping range normally utilized (790-1064 nm). See K. C. Neuman, E. H. Chadd, G. F. Liou, K. Bergman, and S. M. Block, Biophys. J. **77**, 2856 (1999) and the references therein.
28. J. A. Lundqvist, F. Sahlin, M. A. I. Åberg, A. Strömberg, P. S. Eriksson, and O. Orwar, PNAS-USA **95**, 10356 (1998)
29. A. Strömberg, F. Ryttsén, D. T. Chiu, M. Davidson, P. S. Eriksson, C. F. Wilson, O. Orwar, and R. N. Zare, PNAS-USA **97**, 7 (2000)
30. The spatial coincidence of microthermocouples and the focus of an optical trap has been shown to produce temperature jumps greater than 500°C, vaporizing the surrounding media. A method has been developed by which beads of the butyl ester of stearic acid are used to measure the local heating rate due to an optical trap at its focus. See S. C. Kuo, "A simple assay for local meating by optical tweezers," in: *Laser Tweezers in Cell Biology* (*Methods in Cell Biology*, vol. 55) M. P. Sheetz (ed.), pp. 43–45 (Academic Press, Orlando, FL, 1998).
31. D. S. Dimitrov: "Electroporation and electrofusion of membranes," in: *Structure and Dynamics of Membranes (Handbook of Biological Physics*, vol. 1B, series ed. A. J. Hoff), R. Lipowski and E. Sackmann (eds.) pp. 851–901 (Elsevier, Amsterdam, 1995)
32. U. Zimmermann: "Electrofusion and electropermeabilization in genetic engineering," in: *Membrane Fusion*, J. Wilschut and D. Hoekstra (eds.) pp. 665–695 (Marcel Dekker, New York, 1991)
33. J. Teissié and M. P. Rols, "Interfacial membrane alteration associated with electropermeabilization and electrofusion" and A. E. Sowers, "Mechanisms of electroporation and electrofusion," respectively, in: *Guide to Electroporation and Electrofusion*, pp. 139–153 and 119–138 (Academic Press, San Diego, 1992)
34. E. Neumann, "The relaxation hysteresis of membrane electroporation," and G. B. Melikyan and L. V. Chernomordik, "Electrofusion of lipid bilayers," in: *Electroporation and Electrofusion in Cell Biology*, pp. 61–82 and 181–192, respectively (Plenum Press, New York, 1989). The latter develops a cogent hypothesis stating that more complex intermediate structures may exist between the formation of pores and the fusion event. See also L. V. Chernomordik, G. B. Melikyan, and Y. A. Chizmadzhev, Biochim. Biophys. Acta **906**, 309 (1987). Other work has shown that a critical level of permeabilization must exist for fusion to occur when cells are placed in contact. See J. Teissié and C. Ramos, Biophys. J. **74**, 1889 (1998).

35. Consider the simplified case of an insulating spherical membrane containing a conducting aqueous medium. Let this spherical membrane be placed between two parallel plates at a known potential difference. Application of Gauss's law shows that the transmembrane potential has a cos θ dependence. Here θ is the angle between the normals to the bilayer surface at (1) the location of interest and (2) the point where the electric field is perpendicular to the surface. Opposing charges build up on opposite sides within the sphere. Pore formation occurs when a critical breakdown potential for the bilayer is exceeded. The spatial distribution of electroporation has been demonstrated by tracking fluorescent dyes entering [W. Mehrle, U. Zimmermann, and R. Hampp, FEBS Lett. **185**, 89 (1985)] and exiting [D. S. Dimitrov and A. E. Sowers: Biochim. Biophys. Acta **1022**, 381 (1990)] electroporated cells. Optical images showing the spatial distribution of the transmembrane potential during electroporation have been produced in cells by using dyes whose fluorescence depends on the local electric-field strength. See D. Gross, L. M. Loew, and W. W. Webb, Biophys. J. **50**, 339 (1986), and M. Hibino, H. Itoh, and K. Kinosita Jr., Biophys. J. **64**, 1789 (1993).
36. J. Tessié and C. Blangero, Biochim. Biophys. Acta **775**, 446 (1984)
37. Micropipette aspiration to measure the mechanical properties of bilayer membranes was first used to study the elastic properties of sea urchin eggs; J. M. Mitchinson and M. M. Swann, J. Exp. Biol. **31**, 443 and 461 (1954). Since that time this method, or modified forms of it, has been used to study the elastic properties for the membranes of many systems. These systems include, for example, red blood cells [R. P. Rand and A. C. Burton, Biophys. J. **4**, 115 (1964); E. A. Evans, Biophys. J. **13**, 941 (1973)], liposomes [R. Kwok and E. Evans, Biophys. J. **35**, 637 (1981); E. Evans and D. Needham, Faraday Discuss. Chem. Soc. **81**, 267 (1986)], and compartments made of polymer bilayers ("polymersomes") [B. M. Discher, Y. Won, D. S. Ege, J. C. Lee, F. S. Bates, D. E. Discher, and D. A. Hammer, Science **284**, 1143 (1999)].
38. E. Evans: "Physical actions in biological adhesion," in: *Structure and Dynamics of Membranes* (Handbook of Biological Physics, vol. 1B, series ed. A. J. Hoff) R. Lipowsky and E. Sackmann (eds.), pp. 723–754 (Elsevier, Amsterdam, 1995)
39. F. Pincet, W. Rawicz, E. Perez, L. Lebeau, C. Mioskowski, and E. Evans, Phys. Rev. Lett. **79**, 1949 (1997)
40. E. Evans, H. Bowman, A. Leung, D. Needham, and D. Tirrell, Science **273**, 933 (1996)
41. D. V. Zhelev and R. M. Hochmuth, Biophys. J. **68**, 2004 (1995)
42. D. Needham and R. M. Hockmuth, Biophys. J. **55**, 1001 (1989)
43. E. Evans and W. Rawicz, Phys. Rev. Lett. **64**, 2094 (1990)
44. D. E. Discher and N. Mohandas, Biophys. J. **71**, 1680 (1996)
45. D. V. Zhelev, D. Needham, and R. M. Hochmuth, Biophys. J. **67**, 696 (1994)
46. C. F. Wilson, G. J. Simpson, D. T. Chiu, A. Strömberg, O. Orwar, N. Rodriguez, and R. N. Zare, Anal. Chem. **73**, 787 (2001)